

# The Age of the Solar Neighbourhood

James Binney, Walter Dehnen and Gianpaolo Bertelli

*Theoretical Physics, University of Oxford, Oxford, OX1 3NP*

## ABSTRACT

High-quality Hipparcos data for a complete sample of nearly 12 000 main-sequence and subgiant stars, together with Padua isochrones, are used to constrain the star-formation history of the solar neighbourhood and the processes that stochastically accelerate disk stars. The velocity dispersion of a coeval group of stars is found to increase with time from  $\sim 8 \text{ km s}^{-1}$  at birth as  $t^{0.33}$ . In the fits, the slope of the IMF near  $1 M_{\odot}$  proves to be degenerate with the rate at which the star-formation rate declines. If the slope of the IMF is to lie near Salpeter's value,  $-2.35$ , the star-formation rate has to be very nearly constant. The age of the solar neighbourhood is found to be  $11.2 \pm 0.75 \text{ Gyr}$  with remarkably little sensitivity to variations in the assumed metallicity distribution of old disk stars. This age is only a Gyr younger than the age of the oldest globular clusters when the same isochrones and distance scale are employed. It is compatible with current indications of the redshift of luminous galaxy formation only if there is a large cosmological constant. A younger age is formally excluded because it provides a poor fit to the number density of red stars. Since this density is subject to a significantly uncertain selection function, ages as low as 9 Gyr are plausible even though they lie outside our formal error bars.

**Key words:** Milky Way: stellar kinematics, stellar evolution, star formation

## 1 INTRODUCTION

Observations at optical and near-infrared bands have now penetrated to the redshifts  $z \sim 1$  at which it is widely believed that  $L^*$  galaxies formed. The extent and fragility of

a thin galactic disk are such that a disk like the one we inhabit would have been one of the last components to form in a galaxy: the formation of any significant component interior to it would at least have thickened it, and could easily have destroyed it altogether. So it is interesting to ask 'how

old is the solar neighbourhood?

The age of the solar neighbourhood has been estimated in several ways. One method involves comparing measured isotope ratios with values predicted by nucleosynthesis theory and radioactive decay rates. Such studies can only place a lower limit on the age of the solar neighbourhood because the samples studied are unlikely to be as old as the oldest objects in the solar neighbourhood. This approach implies that the age of the solar neighbourhood exceeds 9 Gyr (Morell, Källander & Butcher, 1992) and could be as high as 11 Gyr.

A second approach to dating the solar neighbourhood involves identifying the coolest, and therefore oldest, white dwarfs, and estimating their ages by comparing their colours with those predicted by models of white-dwarf cooling. This approach encounters two difficulties: (i) the theory of white-dwarf cooling is complex and liable to error, and (ii) the oldest white dwarfs are the least conspicuous and are easily missed. Several older studies of cool white dwarfs yield ages in the range 6 to 10 Gyr (Bergeron, Ruiz & Legget, 1997), but recent models of cool white dwarfs (Hansen, 1999; Sammon & Jacobson, 1999) suggest that the coolest objects may be bluer than previously thought and may have been missed in older surveys. It is possible that very old white dwarfs have recently been identified through their proper motions in the Hubble Deep Field (Ibata et al., 1999).

A third way to date the solar neighbourhood is to date individual F stars, which have main-sequence lifetimes comparable to the age of the solar neighbourhood. Since the age of a star of given colour and luminosity depends sensitively on its metallicity, this technique requires accurate metallicity estimates for the programme stars, which in practice

causes the available samples to be small and inadequately representative. Using the sample of Edvardsson et al. (1993), Ng & Bertelli (1998) conclude from such a study that the solar neighbourhood contains stars that are at least 15 Gyr old.

A lower limit to the age of the disk can be set by determining the ages of open clusters by fitting their colour-magnitude diagrams to theoretical models. From six old open clusters and Padua isochrones Carraro, Girardi & Chiosi (1999) find the solar neighbourhood to be older than 10 Gyr.

A fifth approach is to study the morphology of the subgiant branch in the solar-neighbourhood colour-magnitude diagram. Since the solar neighbourhood, unlike a globular cluster, contains stars that are widely spread in both age and metallicity, the sequences in its colour-magnitude diagram are broad and hard to characterize (see Fig. 1). None the less, Jimenez, Flynn & Kotoneva (1998) used this approach to place a lower limit of 8 Gyr on the age of the solar neighbourhood.

Here we date the solar neighbourhood by a new, sixth approach, in which the local colour-magnitude diagram is combined with kinematic information. It has long been known that older populations of solar-neighbourhood stars have larger velocity dispersions (Parenago, 1950; Roman, 1954), and this effect gives rise to the phenomenon called Parenago's discontinuity: when stellar velocity dispersion  $\sigma$  is plotted against a quantity that is related to mean stellar age, for example  $B - V$ , the slope of the graph changes discontinuously near  $B - V = 0.6$  (Fig. 2), because redward of the discontinuity one observes stars of every age, while blue-

ward of it one observes only the more recently formed stars. The Hipparcos Catalogue has made it possible to quantify this phenomenon with unprecedented precision (Binney et al 1997; Dehnen & Binney, 1998), and we show in this paper that it enables us to obtain from the theory of stellar evolution an age for the solar neighbourhood whose precision is comparable to those claimed for the ages of globular clusters.

In addition to determining the solar neighbourhood's age, we constrain both the star-forming history of the solar neighbourhood, and the way in which non-axisymmetric features in the Galactic potential cause the random velocities of stars to increase with age.

In Section 2 we describe the data and the models. Section 3 presents the results of the fits, Section 4 discusses their implications and Section 5 sums up.

## 2 DATA AND MODELS

### 2.1 The data

Figs 1 and 2 show, for the photometrically complete sample of 11 865 Hipparcos stars that is described in Dehnen & Binney (1998; hereafter Paper I), the colour-magnitude diagram and a plot of velocity dispersion versus  $B - V$ . The quantity  $S$  plotted in Fig. 2 is the rms dispersion in proper motion within each bin in  $B - V$ . Hence its relation to the principal velocity dispersion  $\sigma_R$ ,  $\sigma_\phi$  and  $\sigma_z$  depends on the distribution of stars on the sky, which is not precisely uniform (see Fig. 2 of Dehnen 1998). However, for most bins we have

$$S \simeq \left[ \frac{2}{3} (\sigma_R^2 + \sigma_\phi^2 + \sigma_z^2) \right]^{1/2} \quad (1)$$

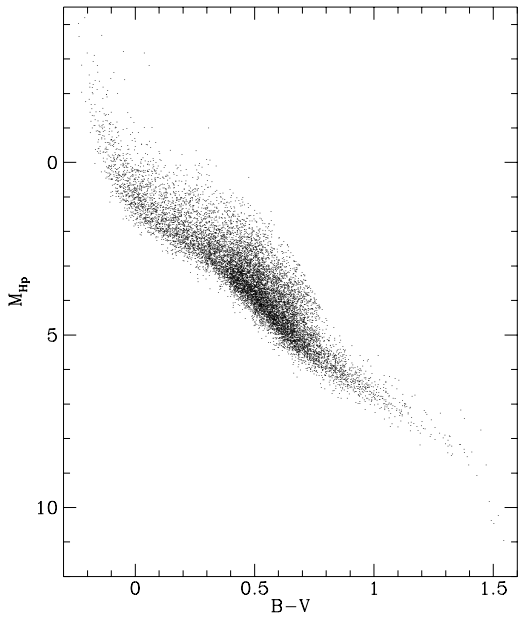


**Figure 1.** Colour-magnitude diagram of the sample.

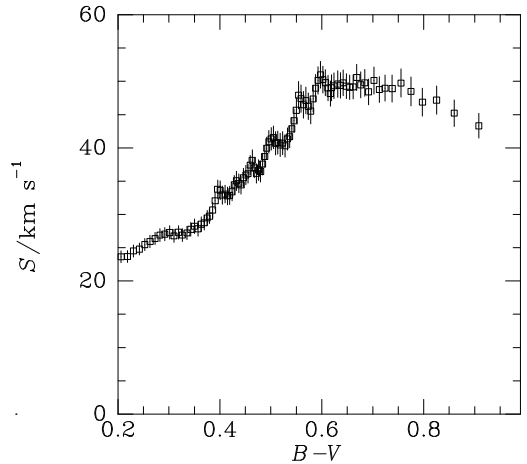


**Figure 2.** The dispersion in proper motions  $S$  of main-sequence stars as a function of dereddened  $B - V$ . The sharp change in gradient near  $B - V = 0.6$  is Parenago's discontinuity.

The data presented in Fig. 2 differ from those shown in Fig. 1 of Paper I in two ways. First, each star has been dereddened by an amount proportional to its distance:

$$E(B - V) = 0.53 (d/\text{kpc}) \quad (2)$$

from Binney & Merrifield (1998), eq. (3.66). Second, the values of  $S$  shown here are for a sliding window whose width varies such that there are always 500 stars in the window. Since a fresh point is plotted each time 100 stars have left

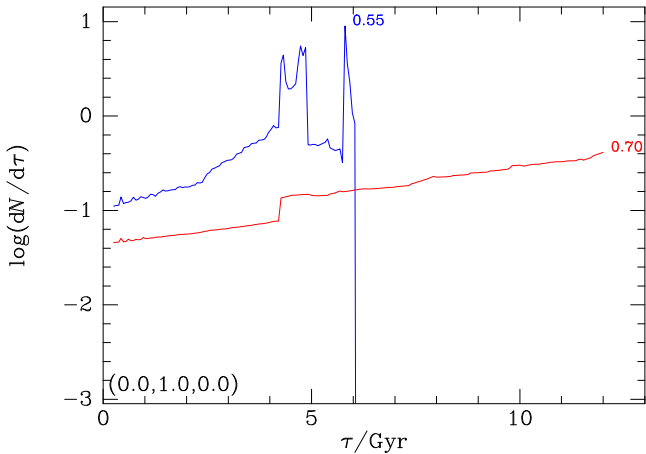


**Figure 3.** The distributions, for  $Z = 0.014$ , over age of stars at  $B - V = 0.5$  and  $B - V = 0.55$ . The solar-neighbourhood has been assumed to be 12 Gyr old and the decay constant of the star-formation rate has been set to  $t_0 = 10$  Gyr.

the window, every fifth point is statistically independent of it predecessors.

## 2.2 The models

We assume that star formation has at all times been characterized by a power-law IMF. Deviation of the actual IMF from power-law form should be unimportant over the narrow range of stellar masses ( $0.8 \lesssim \mathcal{M}/M_\odot \lesssim 2$ ) of interest here. The star-formation rate is assumed to decline exponentially in time with characteristic rate constant  $\gamma$ . These assumptions imply that in a volume-limited sample the distribution of main-sequence stars over mass and age  $\tau$  is

$$\frac{d^2N}{d\mathcal{M}d\tau} \propto \begin{cases} \mathcal{M}^{-\alpha} \exp(\gamma\tau) & \text{for } \tau < \tau_{\max}(\mathcal{M}), \\ 0 & \text{otherwise,} \end{cases} \quad (3)$$

where  $\tau_{\max}(\mathcal{M})$  is the main-sequence lifetime of a star of initial mass  $\mathcal{M}$ .

Our sample is volume-limited for stars more luminous than  $\sim 5 L_\odot$  because these stars lie above the sample's approximate magnitude limit ( $V \sim 8$ ) at the distance,  $d \sim 100$  pc at which their parallaxes become too unreliable to be included in the sample. For less luminous stars,

the sample is effectively apparent-magnitude limited and equation (3) has to be modified by introducing a factor  $\phi$  that is proportional to the volume surveyed. Clearly, in the magnitude-limited regime,  $\phi$  is proportional to  $L^{3/2}$ . Hence we model the distribution of stars in the sample to be

$$\frac{d^2N}{d\mathcal{M}d\tau} \propto \begin{cases} \phi \mathcal{M}^{-\alpha} \exp(\gamma\tau) & \text{for } \tau < \tau_{\max}(\mathcal{M}), \\ 0 & \text{otherwise,} \end{cases} \quad (4a)$$

where

$$\phi(\mathcal{M}, t) = \begin{cases} (L/5 L_\odot)^{3/2} & \text{for } L < 5 L_\odot \\ 1 & \text{otherwise.} \end{cases} \quad (4b)$$

We are interested in the distribution over age of stars

of a given colour  $C$ . This is given by

$$\begin{aligned} \frac{dN}{d\tau} \Big|_{C_0} &\propto \int d\mathcal{M} \delta[C(\mathcal{M}, \tau) - C_0] \frac{d^2N}{d\mathcal{M}d\tau} \\ &\propto \frac{\phi \mathcal{M}^{-\alpha} \exp(\gamma\tau)}{|(\partial C/\partial \mathcal{M})_\tau|} \end{aligned} \quad (5)$$

Thus, to proceed further we require  $(\partial C/\partial \mathcal{M})_\tau$ , the rate of change of colour with mass at a given age, which is in principle readily obtained from the appropriate isochrone. We have used the Padua isochrones of Bertelli et al (1994) for metallicities  $Z = 0.02$ ,  $Z = 0.014$  and  $0.008$ . Since the data are restricted to stars on or near the ZAMS, we cut each isochrone off above the point at which it is 1.8 mag more luminous than the ZAMS at the same colour.

Several technical problems arise in the determination of  $(\partial C/\partial \mathcal{M})_\tau$  from a set of isochrones. First, isochrones are available only at certain times. From these we estimate the isochrone for any given time by interpolation between the isochrones for the closest time before and the closest time after the desired time. Let  $C^-(\mathcal{M}^-)$  be the colour for mass  $\mathcal{M}^-$  at the earlier time. Then we seek the colour  $C^+$  at the later time of the star that has mass

$$\mathcal{M}^+ = \mathcal{M}_{\min} + \frac{\mathcal{M}^- - \mathcal{M}_{\min}}{\mathcal{M}_{\max}^- - \mathcal{M}_{\min}} (\mathcal{M}_{\max}^+ - \mathcal{M}_{\min}), \quad (6)$$

where  $\mathcal{M}_{\min}$  is the mass at which all isochrones start and  $\mathcal{M}_{\max}^{\pm}$  is the mass at which the earlier/later isochrone is truncated. Having located  $C^{\pm}$  and  $\mathcal{M}^{\pm}$  we linearly interpolate between them in time to obtain  $C(\mathcal{M})$  at the desired time.

Once an isochrone has been constructed for a given time, we normally obtain the average of  $|\partial C/\partial \mathcal{M}|^{-1}$  over each colour bin by analytically integrating over the quadratic in  $\mathcal{M}$  that passes through three appropriate points on the isochrone; this procedure yields a finite value even when  $(\partial C/\partial \mathcal{M})$  vanishes in the range of integration. Unfortunately, isochrones often show poorly-sampled sharp turnings. At such points the quadratic that passes through the data points can be unphysical and we have deemed it wiser to obtain the average of  $|\partial C/\partial \mathcal{M}|^{-1}$  from linear approximations to  $C(\mathcal{M})$ .

Fig. 3 shows, for metallicity  $Z = 0.014$  ( $[\text{Fe}/\text{H}] = -0.155$ ), the distributions over age for two colours, namely  $B - V = 0.55$  and  $B - V = 0.7$ . At the bluer colour, all stars are younger than 6.1 Gyr, while at the redder colour, which lies redward of Parenago's discontinuity, there are stars of every age up to the assumed age of the disk, 11 Gyr. Both distributions are sharply peaked in age. The step at age  $\tau = 4.2$  Gyr in the distribution for  $B - V = 0.7$  arises because isochrones older than 4.2 Gyr cross  $B - V = 0.7$  twice, once on the main sequence and once on the subgiant branch. The peaks at  $\tau = 4.5$  Gyr in the distribution for  $B - V = 0.55$  are associated with times at which the main-sequence turnoff lies near  $B - V = 0.55$  and  $(\partial C/\partial \mathcal{M})$  vanishes at this colour.

The age distribution at a given colour depends strongly on the metallicity of the isochrones employed. In reality

the metallicities of solar-neighbourhood stars cover a band of finite width. The observational characterization of this band has been hampered by the want of an unbiased sample of disk stars with accurately determined metallicities. However, data from Pagel & Patchett (1975), Rana & Basu (1990), Rocha-Pinto & Maciel (1996) and Flynn & Morell (1998) suggest that the band is centred on  $[\text{Fe}/\text{H}] \simeq -0.15$  and is  $\sim 0.5$  dex wide (cf. Fig. 7 of Flynn & Morell). We crudely simulate the band with a sum of three Dirac delta-functions in metallicity at  $[\text{Fe}/\text{H}] = -0.4, -0.15$  and 0 with respective weights 0.25, 0.5 and 0.25. Table 1 gives, for this metallicity mixture and a constant star-formation rate, the distribution in age of the stars that would be picked up in each of three colour bands. The bands, which are all 0.1 mag wide in  $B - V$ , lie, respectively, blueward of Parenago's discontinuity (central  $B - V = 0.4$ ), across the discontinuity (central  $B - V = 0.6$ ) and redward of it (central  $B - V = 0.8$ ).

The theory of stellar scattering has been examined many times; we refer the reader to §7.5 of Binney & Tremaine (1987) for an elementary discussion and to Jenkins (1992) for an up-to-date treatment and references to the literature. In the simplest models, the stellar velocity dispersion increases as some power of time,  $\sigma \sim t^{\beta}$ , with  $0.2 \lesssim \beta < 0.5$ , and we assume such a power-law dependence here. Specifically, we take the velocity dispersion  $S$  of a group of stars of known age distribution to be given by

$$S^2 = \frac{\int_0^{\tau_{\max}} d\tau (dN/d\tau) \{v_{10}[(\tau + \tau_1)/(10 \text{ Gyr} + \tau_1)]^{\beta}\}^2}{\int_0^{\tau_{\max}} d\tau (dN/d\tau)} \quad (7)$$

In this formula  $\tau_{\max}$  is the age of the solar neighbourhood,  $\tau_1$  controls the random velocity of stars at birth, and  $v_{10}$  and  $\beta$  characterize the efficiency of stellar acceleration.

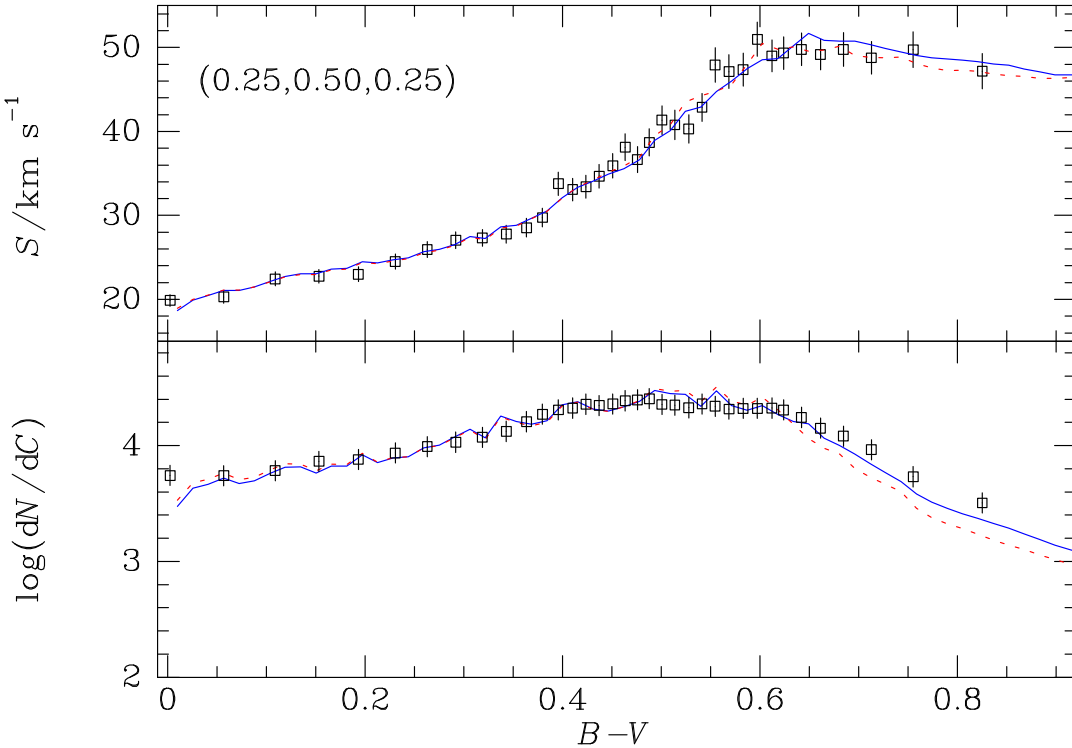


**Figure 4.** Top panel: data from Fig. 2 together with two model fits. The full (dashed) curve is for the model whose parameters are given in the top (bottom) row of Table 2. The solar-neighbourhood metallicity distribution is taken to be the sum of three Dirac delta functions at  $Z = 0.008$ ,  $Z = 0.014$  and  $Z = 0.02$  with weights 0.25, 0.5 and 0.25, respectively. Lower panel: the corresponding fits to the number of stars in each colour bin.

**Table 1.** The distribution over age  $\tau$  of stars in three colour bands. Each band is 0.1 mag wide in  $B - V$ .

$\tau$	$(0.35 - 0.45)$	$(0.55 - 0.65)$	$(0.75 - 0.85)$
0.50	23.30	4.79	1.36
1.00	30.40	4.95	1.35
1.50	71.36	5.17	1.35
2.00	67.05	5.83	1.35
2.50	18.98	9.70	1.35
3.00	10.66	13.67	1.35
3.50	8.21	15.61	1.35
4.00	1.03	13.84	1.31
4.50	0.03	17.05	1.34
5.00	0.00	24.06	1.37
5.50	0.00	21.55	1.50
6.00	0.00	21.25	1.59
6.50	0.00	18.44	1.61
7.00	0.00	16.68	1.60
7.50	0.00	11.57	1.61
8.00	0.00	24.20	1.62
8.50	0.00	16.98	1.88
9.00	0.00	13.97	2.06
9.50	0.00	9.91	2.18
10.00	0.00	8.82	2.33

### 3 FITS TO THE DATA

The data are of two types. The data plotted in Fig. 2 constrain the parameters,  $\beta$ ,  $v_{10}$ ,  $\tau_1$  and  $\tau_{\max}$  that characterize

the stochastic acceleration process, but give little leverage on the parameters  $\alpha$  and  $\gamma$  that parameterize the disk's star-formation history. The last two parameters are, however, strongly constrained by the number of stars in each colour bin. Hence, we use the Levenberg–Marquardt nonlinear least-squares algorithm (Press et al 1986) to minimize the sum of the  $\chi^2$  values of the model's fits to both the numbers of stars and the velocity dispersion of each colour bin.

Only every fifth of the data points plotted in Fig. 2 is statistically independent, so we have fitted to only a subset of the data. When only every fifth data point was employed, to ensure that all the data points used were statistically independent and  $\chi^2$ -values were easily interpreted, the results proved to depend significantly on *which* subset of the data were used. More nearly consistent results are obtained when

every third data point is employed, so that every data point is statistically independent of its second-nearest neighbours. The results reported here are for this case. Hence,  $\chi^2$ -values can be expected to be lower than those one would obtain for statistically independent data points.

The first three rows of Table 2 show the parameters of three fits to the data that differ in the assumed metallicity composition of the solar neighbourhood: the first row is for weightings (0.25, 0.5, 0.25) of the three metallicity components, while the second and third rows are for (0.333, 0.333, 0.333) and (0.2, 0.6, 0.2), respectively. The differences between values of a given parameter for different assumed metallicities are comparable to or smaller than the formal error in that parameter. Thus, our results are effectively independent of reasonable assumptions about the metallicity of the solar neighbourhood.

The formal error in  $\alpha$  is quite large ( $\sim 25\%$ ). Moreover,  $\alpha$  is strongly correlated with the rate parameter  $\gamma$ : Table 3 shows that the correlation coefficient between these two parameters is nearly unity. This is because increasing  $\gamma$  diminishes the current star-formation rate relative to its historical average, and this makes blue stars relatively scarce. This effect can be effectively cancelled by increasing  $\alpha$  and thus flattening the IMF. The values of  $\alpha$  given in the first three rows of Table 2 are consistent with Salpeter's classical value,  $\alpha = -2.35$ .

Tables 2 and 3 show that the formal error in  $\beta$  is small ( $\sim 0.02$ ), but  $\beta$  is highly correlated with  $\tau_1$ . The formal error in the age of the solar neighbourhood,  $\tau_{\max}$  is  $\sim 0.75$  Gyr and this parameter is not particularly strongly correlated with any other.

The age,  $11.2 \pm 0.75$  Gyr, to which the first three rows of Table 2 point is older than recent models of globular clusters and cosmological developments would lead one to expect (see below). So it is interesting to fix  $\tau_{\max}$  at a younger age and see how well the data can be fitted by varying the other parameters. The bottom row of Table 2 and the dashed curves in Fig. 4 show the result of this exercise when we set  $\tau_{\max} = 9$  Gyr. The value of  $\chi^2$  per degree of freedom has risen from 0.78 when  $\tau_{\max}$  is varied to 0.95. Fig. 4 shows that this increase in  $\chi^2$  is attributable to a deterioration in the fit to the observed density of red stars. In fact, the model with the smaller age gives a slightly better fit to the velocity data plotted in the upper panel of Fig. 4, especially in the crucial region around the discontinuity. Since the fits to the stellar number densities are sensitive to our rather uncertain selection function, the model with  $\tau_{\max} = 9$  Gyr should be considered at least as plausible as the models with older ages.

The deficit of red stars in the model with  $\tau_{\max} = 9$  Gyr arises from two factors: the model has a flat IMF –  $\alpha = -1.74$  – and a star-formation rate that increases with time.

## 4 DISCUSSION

Our approach to the determination of the age of the solar neighbourhood has much in common with the work of Jimenez, Flynn & Kotoneva (1998): we both use samples of Hipparcos stars and stellar evolution as the clock. However, since the sub-giant branch is not evident in Fig. 1, our technique is radically different from that of Jimenez et al., which focused on the morphology of the sub-giant branch. Our results show that by including kinematic information,

**Table 2.** Fitted values of the parameters for four models. The first three rows show fits for different weightings of the metallicity components  $[\text{Fe}/\text{H}] = -0.4, -0.15, 0$ : from top to bottom the weightings are  $(0.25, 0.5, 0.25)$ ,  $(0.333, 0.333, 0.333)$  and  $(0.2, 0.6, 0.2)$ . The fit given by the first row is plotted in Fig. 4. The last row shows the result of fixing  $\tau_{\text{max}} = 9$  Gyr with metallicity weightings  $(0.25, 0.5, 0.25)$ .

$\alpha$	$\beta$	$\gamma/\text{Gyr}^{-1}$	$\tau_{\text{max}}/\text{Gyr}$	$\tau_1/\text{Gyr}$	$v_{10}/\text{km s}^{-1}$
$-2.26 \pm 0.48$	$0.328 \pm 0.021$	$-0.006 \pm 0.046$	$11.16 \pm 0.77$	$0.030 \pm 0.072$	$58.1 \pm 1.4$
$-2.58 \pm 0.47$	$0.327 \pm 0.022$	$-0.035 \pm 0.044$	$11.80 \pm 0.39$	$0.039 \pm 0.074$	$58.0 \pm 1.5$
$-2.14 \pm 0.48$	$0.322 \pm 0.093$	$-0.000 \pm 0.045$	$11.19 \pm 0.74$	$0.006 \pm 0.065$	$57.8 \pm 1.3$
$-1.74 \pm 0.47$	$0.357 \pm 0.024$	$0.075 \pm 0.046$	9.000	$0.107 \pm 0.093$	$59.9 \pm 1.5$

**Table 3.** The normalized covariance matrix,  $\langle \delta p_i \delta p_j \rangle / (\sigma_i \sigma_j)$ , of the model parameters for the six-parameter fit shown by the full curves in Fig. 4 and the first row of Table 2.

	$\alpha$	$\beta$	$\gamma$	$\tau_{\text{max}}$	$\tau_1$
$\beta$	-0.338				
$\gamma$	0.908	-0.322			
$\tau_{\text{max}}$	-0.340	-0.240	-0.491		
$\tau_1$	-0.200	0.910	-0.173	-0.203	
$v_{10}$	-0.570	0.850	-0.581	-0.156	0.615

which provides a means of distinguishing old from young stars, at least in a statistical sense, we can overcome the difficulty that one encounters when one attempts to transfer from globular clusters to the solar neighbourhood a dating technique that relies on the sharpness of sequences in the colour-magnitude diagrams of globular clusters. Our final age estimate,  $11.2 \pm 0.75$  Gyr, is compatible with the constraint that Jimenez et al. derive,  $\tau_{\text{max}} > 8$  Gyr.

In addition to its cited 0.75 Gyr formal error, our estimate of the age of the solar neighbourhood is subject to any systematic error in the isochrones we have employed. Great strides have been taken by stellar evolution models within the last decade, largely as a result of upgrades to the atomic physics used. In particular, there is now good agreement between observation and theory in the pulsation periods of variable stars (Chiosi et al. 1992). Also, models produced by different groups are in excellent agreement with one another, especially when convective overshoot is unimportant, as is in the case of main-sequence stars older than  $\sim 6$  Gyr. The

remaining discrepancies between the isochrones of different groups are principally due to different transformations between effective temperature and colours such as  $B - V$ . In this connection it is noteworthy that displacing our solar-metallicity isochrones for 8, 11 and 15 Gyr by 0.05 mag to the blue yields almost perfect agreement with the isochrones of Jimenez et al. near the crucial turn-off. When the velocity-dispersion data are fitted with such displaced isochrones,  $\tau_{\text{max}}$  increases by 3 to 4 Gyr depending on the assumed metallicity distribution.

The difference between our solar-neighbourhood age and the ages of globular clusters should be less subject to systematic error than an absolute age. Gratton et al. (1997) have determined the ages of globular clusters by fitting the absolute magnitude,  $M_V(\text{TO})$  of the main-sequence turnoff to the isochrones of different groups. The Bertelli et al. (1997) isochrones yielded the youngest ages, ranging up to 12.4 Gyr for NGC 6341. Hence, by this reckoning, the solar neighbourhood is only one Gyr younger than an old globular cluster. Weight is lent to this conclusion by the fact that Gratton et al. determined  $M_V(\text{TO})$  by forcing the cluster main-sequences to pass through the locations of sub-dwarfs of appropriate metallicity for which Hipparcos had determined a parallax. Hence, we are comparing ages that are

based on the same isochrones and the same distance scale. If the comparison is misleading, it will be because our age of the solar neighbourhood relies on the colour calibration of the Bertelli et al. isochrones, whereas that of Gratton et al. was designed to be largely free from this calibration. Note, however, that shifting the calibration in the sense suggested by the work of Jimenez would make the solar neighbourhood older than the oldest globular clusters.

As Table 2 illustrates, the parameters  $\beta$ ,  $\tau_{\max}$ ,  $\tau_1$  and  $v_{10}$  that characterize the age of the disk and the stochastic acceleration of stars, are remarkably well determined by the models. The exponent  $\beta$  lies in the range expected if the acceleration process is primarily driven by spiral structure and modulated by stars scattering off giant molecular clouds (Jenkins 1992). Our allowed range,  $\beta = 0.33 \pm 0.03$ , excludes the value  $\beta = 0.5$  that has been advocated by Wielen (Wielen, 1977; Wielen, Fuchs & Dettbarn 1996). Notice that for  $\beta = \frac{1}{3}$  and  $v_{10} = 58 \text{ km s}^{-1}$ , equation (7) predicts that the velocity dispersion of stars at birth is  $8.4 \text{ km s}^{-1}$  for  $\tau_1 = 0.03 \text{ Gyr}$ . For comparison, spiral structure endows molecular clouds with non-circular velocities  $\sim 7 \text{ km s}^{-1}$  (Malhotra, 1995), while the internal velocity dispersions within molecular clouds are  $\sim 3 \text{ km s}^{-1}$  (Solomon & Rivolo, 1989). Hence  $8.4 \text{ km s}^{-1}$  implies that during formation stars acquire slightly larger random velocities than the gas from which they formed had.

The degeneracy between  $\alpha$  and  $\gamma$  that is quantified by Table 3 has been thoroughly discussed by Haywood, Robin & Crézé (1997a). These authors point out that  $\alpha$  and  $\gamma$  are connected not only with one another, but also with the vertical structure of the disk, because older and less lumi-

nous stars form a thicker disk than young and luminous stars, so the latter tend to be over-represented in solar-neighbourhood samples. In fact, the value of  $\alpha$  returned by our fits is sensitive to the selection function  $\phi$  that we adopt, and this is not as well defined as we would like because, the sample, in common with virtually all Hipparcos samples, involves complex selection criteria. In particular, our primary selection criterion is by relative parallax error. This error is primarily a function of distance, but it has non-negligible dependence on both ecliptic latitude and apparent magnitude. Early-type stars will tend to be included to greater distances than late-type stars.

In a second paper Haywood, Robin & Crézé (1997b) exploit the connection with the disk's vertical structure by constraining their models of the disk's evolution with both local data and faint star counts at the Galactic poles. They find that these fits favour a flat IMF and a constant or increasing star-formation rate, very much in line with the result of our fits to the data. This conclusion is in marked contrast with that reached by Scalo (1986), who found that in the relevant mass range ( $0.8 M_{\odot} \lesssim M \lesssim 2 M_{\odot}$ ) the slope of the IMF is flattening from  $\alpha \sim -3.3$  at  $M > M_{\odot}$  to  $\alpha \sim -1.8$  at  $M < M_{\odot}$ , and with the conclusion of Kroupa, Tout & Gilmore (1993), who found that the IMF is as steep as  $\alpha = -4.5$  for  $M > M_{\odot}$  and has  $\alpha \sim -2.2$  below  $M_{\odot}$ . Unfortunately, the strength of the correlation between  $\alpha$  and  $\gamma$  in our fits prevents us from throwing significant weight behind one side or the other in this controversy.

We should also remark that the physical meaning of the parameters  $\alpha$  and  $\gamma$  used here may differ slightly from the meaning of the corresponding parameters in other studies.

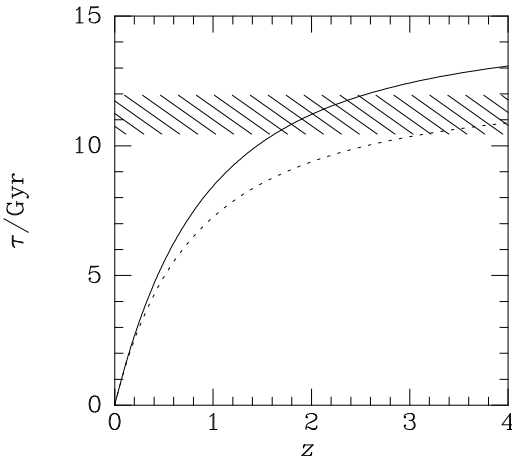


**Figure 5.** The full curve shows the relationship between redshift and time for  $H_0 = 65 \text{ km s}^{-1} \text{ Mpc}^{-1}$ ,  $\Omega_{\text{matter}} = 0.3$  and  $\Omega_{\Lambda} = 0.7$ . The dashed curve is for the same parameter values except  $\Omega_{\Lambda} = 0$ . The  $1\sigma$ -error band of our determination of the age of the solar neighbourhood is shaded.

Since stars can diffuse into and out of the volume that was surveyed by Hipparcos, the derivative with respect to age of the density of stars of a given type will strictly differ from the rate at which such stars formed at the corresponding time in the past. For example, the thickness of the disk increases with age, so the density of objects near the plane, where Hipparcos observed, will increase with  $\tau$  less rapidly than the true star-formation rate did. Radial diffusion of stars could have a similar effect, and these effects will slightly reduce the magnitude of the measured value of  $\gamma$ .

There is currently much interest in determining the redshift at which galactic disks such as our own formed. What redshift does an age of 11.2 Gyr correspond to? The full curve in Fig. 5 shows the redshift–age relationship in the currently popular  $\Omega_{\text{matter}} = 0.3$ ,  $\Omega_{\Lambda} = 0.7$  cosmology for  $H_0 = 65 \text{ km s}^{-1} \text{ Mpc}$ , together with the formal  $1\sigma$ -error band of our age determination. The lower edge of this band crosses the age– $z$  relation at  $z = 1.6$ , which is on the high side of current estimates of the redshift at which  $L^*$  disks such as that of the Milky Way formed (Baugh et

al., 1998; Madau, Pozzetti & Dickinson, 1998). The dashed curve shows the redshift–age relationship for the same Hubble constant and  $\Omega_{\text{matter}}$  but vanishing cosmological constant. This curve enters our possible age band at  $z = 3.1$ , which considerably exceeds the redshift at which  $L^*$  disks are believed to form. Hence, our age estimate is compatible with  $H_0 = 65 \text{ km s}^{-1} \text{ Mpc}^{-1}$  only if the cosmological constant is currently important. If  $H_0$  were as small as  $55 \text{ km s}^{-1} \text{ Mpc}^{-1}$ , the redshift–age relation would be compatible with our age estimate for both  $\Omega_{\Lambda} = 0.7$  (when  $z_{\text{formation}} \gtrsim 1.1$ ) and  $\Omega_{\Lambda} = 0$  (when  $z_{\text{formation}} \gtrsim 1.7$ ).

Fig. 5 shows that combining the evidence that  $L^*$  disks formed at  $z \sim 1$  with either of the cosmological models that have  $H_0 = 65 \text{ km s}^{-1} \text{ Mpc}^{-1}$  leads to the conclusion that the solar neighbourhood should be  $\sim 9$  Gyr old. Fig. 4 shows that such a low value of  $\tau_{\text{max}}$  is formally excluded because it yields a poor fit to the number density of stars, even though it provides an excellent fit to the velocity data. Since the model stellar densities are subject to a significantly uncertain selection function, a low value of  $\tau_{\text{max}}$  that is compatible with  $H_0 = 65 \text{ km s}^{-1} \text{ Mpc}^{-1}$  and  $\Omega_{\Lambda} = 0$  should not be regarded as excluded despite the formal error bars on our age determination.

## 5 CONCLUSIONS

By fitting a set of high-quality Hipparcos data with state-of-the-art isochrones we have jointly constrained the star-formation history of the solar neighbourhood and the mechanism that stochastically accelerates stars. The value we obtain for the slope of the IMF near  $1 M_{\odot}$  is compatible with the classical Salpeter value, but the uncertainty of this pa-

parameter is large because an increase or decrease of it can be almost perfectly compensated by a change in the time constant that quantifies the decline in the star formation rate. If the slope of the IMF is to lie near Salpeter's value, the star formation rate has to be almost constant in time. A good fit to the data is obtained by assuming that the velocity dispersion of a coeval group of stars increases from  $\sim 8 \text{ km s}^{-1}$  as  $t^\beta$  with  $\beta = 0.33 \pm 0.02$ . The age of the solar neighbourhood is found to be  $11.2 \pm 0.75 \text{ Gyr}$ , which is slightly older than currently popular values of the cosmological constants and likely redshifts for the formation of massive stellar disks would predict. A younger age for the solar neighbourhood,  $\sim 9 \text{ Gyr}$  that is suggested with cosmological considerations is formally excluded because it provides a poor fit to the number density of red stars. Since this number density is subject to a significantly uncertain selection function, such young ages cannot be considered to have been securely excluded.

## ACKNOWLEDGMENTS

We thank M.G. Edmunds for valuable comments on the first version of this paper.

## REFERENCES

Baugh C., Cole C., Frenk C., Lacey C., 1998, *ApJ*, 498, 504

Bergeron J., Ruiz M.T., Legget S.K., 1997, *ApJS*, 108, 339

Bertelli G., Bressan A., Chiosi C., Fagotto F., Nasi E., 1994, *A&AS*, 106, 275

Binney J.J., Dehnen W., Houk N., Murray C.A., Penston M.J., 1998, in "Hipparcos - Venice 1997," ed. B. Battrick, ESA, Noordwijk, p. 473

Binney J.J., Tremaine S.D., 1987, "Galactic Dynamics", Princeton University Press, Princeton

Carraro G., Girardi L., Chiosi C., 1999, *MNRAS*, 309, 430

Chiosi C., Wood P., Bertelli G., Bressan A., 1992, *ApJ*, 387, 320

Dehnen W., 1998, *AJ*, 115, 2384

Dehnen W., Binney J.J., 1998, *MNRAS*, 298, 387

Flynn C., Morell O., 1997, *MNRAS*, 286, 617

Gratton R.G., Pecci F.F., Carretta E., Clementini G., Corsi C.E., Lattanzi M., 1997, *ApJ*, 491, 749

Hansen B., 1999, *ApJ*, 520, 680

Haywood M., Robin A.C., Crézé M., 1997a, *A&A*, 320, 428

Haywood M., Robin A.C., Crézé M., 1997b, *A&A*, 320, 440

Ibata R.A., Richer H.B., Gilliland R.L., Scott D., 1999, *ApJ*, 524, 95

Jenkins A., 1992, *MNRAS*, 257, 620

Jimenez R., Flynn C., Kotoneva E., 1998, *MNRAS*, 299, 515

Jimenez R., Thejll P., Jorgensen U.G., MacDonald J., Pagel B., 1996, *MNRAS*, 282, 926

Kroupa P., Tout C.A., Gilmore G., 1993, *MNRAS*, 262, 545

Malhotra S., 1994, *ApJ*, 433, 687

Ng Y.K., Bertelli G., 1998, *A&A*, 329, 943

Morell O., Källander D., Butcher H.R., 1992, *A&A*, 259, 543

Pagel B.E.J., Patchett B.E., 1975, *MNRAS*, 172, 13

Parenago P.P., 1950, *astron. Zhur.*, 27 150

Madau P., Pozzetti L., Dickinson M., 1998, *ApJ*, 498, 106

Press W.H., Flannery, B.P., Teukolsky A.A., Vetterling W.T., 1986, "Numerical Recipes", Cambridge University Press, New York

Rana N.C., Basu S., 1990, *Ap&SS*, 168, 317

Rocha-Pinto H.J., Maciel W.J., 1996, *MNRAS*, 279, 447

Roman N.G., 1954, *AJ*, 59, 307

Saumon D., Jacobson S., 1999, *ApJ*, 511, L107

Scalo J.M., 1986, *Fundam. Cosmic Physics*, 11, 1

Solomon P.M., Rivolo A.R., 1989, *ApJ*, 339, 919

Wielen R., 1977, A&A, 60, 263

Wielen R., Fuchs B., Dettbarn C., 1996, A&A, 314, 438

This paper has been produced using the Royal Astronomical Society/Blackwell Science Te<sub>X</sub> macros.